

29. Zeilinger, A., Horne, M. A., Weinfurter, H. & Zukowski, M. Three particle entanglements from two entangled pairs. *Phys. Rev. Lett.* **78**, 3031–3034 (1997).
30. Zukowski, M., Zeilinger, A. & Weinfurter, H. Entangling photons radiated by independent pulsed source. *Ann. NY Acad. Sci.* **755**, 91–102 (1995).

Acknowledgements

We thank D. M. Greenberger, M. A. Horne and M. Zukowski for useful discussions. This work was supported by the Austrian Fonds zur Förderung der Wissenschaftlichen Forschung, the Austrian Academy of Sciences and the Training and Mobility of Researchers programme of the European Union.

Correspondence and requests for materials should be addressed to A.Z. (e-mail: Zeilinger-office@exp.univie.ac.at).

Ball lightning caused by oxidation of nanoparticle networks from normal lightning strikes on soil

John Abrahamson & James Dinniss

Chemical and Process Engineering Department, University of Canterbury, Private Bag 4800, Christchurch, New Zealand

Observations of ball lightning have been reported for centuries, but the origin of this phenomenon remains an enigma. The ‘average’ ball lightning appears as a sphere with a diameter of 300 mm, a lifetime of about 10 s, and a luminosity similar to a 100-W lamp¹. It floats freely in the air, and ends either in an explosion, or by simply fading from view. It almost invariably occurs during stormy weather^{2,3}. Several energy sources have been proposed^{2–4} to explain the light, but none of these models has succeeded in explaining all of the observed characteristics. Here we report a model that potentially accounts for all of those properties, and which has some experimental support. When normal lightning strikes soil, chemical energy is stored in nanoparticles of Si, SiO or SiC, which are ejected into the air as a filamentary network. As the particles are slowly oxidized in air, the stored energy is released as heat and light. We investigated this basic process by exposing soil samples to a lightning-like discharge, which produced chain aggregates of nanoparticles; these particles oxidize at a rate appropriate for explaining the lifetime of ball lightning.

Away from buildings, the material most commonly in the path of a lightning strike is a tree, and then soil. Lightning leaves solid tubular or lumpy residues (fulgurites) after interacting with sand or soil, which indicate that the discharge has penetrated beneath the ground surface, and that the material has been molten. If soils or tree roots are regarded as a fine mixture of silica and carbon, then under such high-temperature treatment, one expects chemical reduction to silicon metal, silicon monoxide, or silicon carbide, followed by oxidation by oxygen from the air.

Such reduction of a C/SiO₂ mix using an electric arc is commonly used in industry. Liquid silicon is the dominant equilibrium condensed phase around 3,000 K (ref. 5) for C/SiO₂ mole ratios of 1–2, with solid SiC expected for ratios >2. This ratio can range from 0.1 to about 2 for mineral soils, and is much higher for wood. Silicon metal has been observed⁶ in the silicate glass deposit adjacent to a charred tree root after a large lightning strike.

Such fast-cooling processes often yield nanometre-sized particles^{7,8}. For lightning action on a soil, or a soil/wood mix with a C/SiO₂ ratio of 1–2, we expect the particles to be Si and SiO

(formed by condensation of the dominant vapour species⁵), with SiC and soot dominating for C/SiO₂ > 2. Most nanoparticle suspensions are found in the form of chain aggregates⁹, which extend where charged particles influence their neighbours¹⁰ (in conditions of higher particle charge and numbers, and fewer gaseous ions, as at cooler flame temperatures). Charge on the growing chain may induce a dendrimer-like structure, growing from the centre. The possible size is suggested by the following observations in quiescent air. Filamentary particle structures spanning 50 mm have been found¹¹ after vaporizing metal in air in the presence of electric fields. Early work with charged aerosols¹² showed the formation of a spherical networked aerosol suspension of diameter 200 mm.

Particle networks have been proposed more recently¹³ as a general basis for ball lightning, with the aggregation influenced by the field of the growing ball¹, but without a clear proposal for the chemical reaction occurring. Oxidation of copper particles has also been suggested¹⁴, but with this process occurring at the perimeter of the sphere of air carrying the particles: a network structure or rate limitation at the particle surface was not mentioned.

A Si/SiO/SiC nanoparticle network would have a large surface, and could be expected to oxidize rapidly, even explosively. However, we emphasize that the rate of oxidation would be limited by the need for oxygen to diffuse through the developing SiO₂ layer to the metal (or carbide) beneath. Laboratory oxidation studies on silicon surfaces^{15,16} show that both oxygen and water are reactants. Whether oxygen or water dominate the reaction with silicon depends on their partial pressures. SiC oxidizes at a similar rate to Si (ref. 17).

We checked for the existence of nanosphere chains after exposing soil to a lightning-like discharge. A 10–20 kV d.c. discharge penetrated a 3-mm layer of soil, transferring up to 3.4 C of charge. Sampling of the air space close to the discharge caused deposits to form on a glass-fibre filter and a filter-mounted transmission electron microscope (TEM) grid. Examination of these deposits using scanning electron microscopy (SEM) showed ‘lumpy’ filament links (width 100 nm, length 10 μm) between the glass fibres. TEM at high resolution (Fig. 1) showed chain aggregates of nanospheres, 5–70 nm in diameter. Larger spheres, several micrometres in diameter, were collected on all the filters, and were collectively of similar mass to the nanoparticles.

Despite using charge transfer within the range observed for lightning strikes¹⁸, we did not observe any luminous ball. At the higher power levels, the soil sample was always completely blown away in the radial direction. It appeared unlikely that a network of delicate long filaments could survive the discharge shockwave. If the

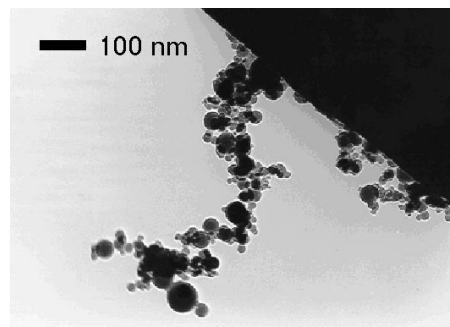


Figure 1 Transmission electron micrograph of nanoparticle chains sampled from the discharge environment. These particles were deposited on a nickel grid, after sampling the gas space above a 14.9-kV discharge on a silt loam soil containing 12.5% carbon. The soil was placed in a layer on a flat conducting (graphite) base below a vertical graphite electrode, with a gap of 22 mm to the soil, and 3.0 C charge transferred from a 204 μF capacitor. The extended chains are made up of spheres 5–70 nm in diameter; the chain width is 25–125 nm. Six of the highest-power runs were examined in this way, with three soils. All showed similar results, except one showing only larger particles.

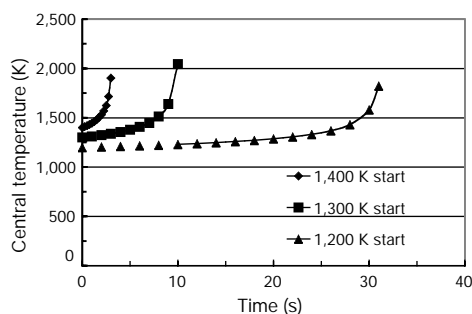


Figure 2 Temperature history of a 300-mm-diameter ball lightning predicted from our nanoparticle network model. The temperature of the central region is given for starting temperatures 1,200, 1,300 and 1,400 K. The ball has 100 g m^{-3} Si loading in 25-nm spheres. Lifetimes before melting are around 30, 10 and 3 s, respectively. For a temperature of 1,473 K, the rate of heat release is estimated at 79.0 kW m^{-2} of ball volume. The rate has been corrected for the partial pressures of O_2 and H_2O , yielding 0.10 nm s^{-1} oxide growth at 1,473 K for either reactant. Estimation for other temperatures uses an activation energy¹⁵ of 189 kJ mol^{-1} .

observed filaments form the basis of ball lightning, they must somehow avoid this shockwave. Lightning strikes to ground penetrate a deeper soil layer than in our experiments. Radial dispersal of vapour/hot particles is then curtailed by the surrounding soil. This hot material from the fulgurite cavity would instead disperse up into the air, after decay of the strike pressure.

This action of a fulgurite cavity has been simulated¹⁹ by an evacuated chamber with an opening to the atmosphere temporarily sealed with a breakable diaphragm. A high voltage discharge acted on the chamber wall materials (ice and plastics), breaking the diaphragm. A luminous spherical ball (150–400 mm dia.) was ejected that persisted for several milliseconds (ref. 19). These observations showed all the features of a “smoke-ring vortex”, the toroidal vortex formed by sudden jetting of a fluid through a circular opening²⁰. The vortex above a fulgurite cavity is expected to form its own spherical quiescent space, thereby allowing formation of delicate filaments. The materials chosen above¹⁹ did not contain metal elements, eliminating any long-lived oxidation and luminosity. Soot nanoparticles from the plastic pyrolysis would oxidize in several milliseconds.

Ball lightning is commonly spherical, and shows elastic behaviour. This is consistent with observed elastic properties of nanoparticle chains⁹. Also, the repulsion of like particle charges will keep the net from collapsing in on itself, with those at the ball surface giving a surface-tension effect to the ball¹, restoring the spherical shape after deformation against solid boundaries. The ball will generally follow the wind but electrical forces (caused by interactions with, for example, nearby conductors) may also be important.

Our quantitative model for a net-filled ball lightning assumes negligible temperature difference between the network and the enclosed gas, and negligible local relative motion between network and gas. The nanoparticle Si concentration can be given a maximum value, around 100 g m^{-3} , derived from vapour Si at 1 atmosphere pressure and 3,000–5,000 K (ref. 5), cooled to around 1,000–1,500 K. The jet from the fulgurite will also pick up an uncertain amount of non-vaporized particles of soil (micrometre-sizes) from the channel sides. By mixing, these will rapidly cool the jet to a particular final temperature. If the ball that forms has neutral buoyancy (as commonly observed), the extra loading of soil is about 800 g m^{-3} . The soil particles are expected to have melted like those observed in our SEM study, and to become attached to the network. They add to the specific heat capacity of the ball. We choose a ball diameter of 300 mm (within the size range of luminous

fulgurite ejection¹⁹, equal to the mean observed size of ball lightning¹).

The transient (symmetrical) temperature profile T within the ball can be evaluated from energy conservation for a thin shell of the ball between radius r and $r + \delta r$ over a time interval δt :

$$(\rho C_p)_{\text{ball}}(4\pi r^2 \delta r) \delta T_{\text{rise}} = (-\delta(4\pi r^2 q) + H(4\pi r^2 \delta r)) \delta t \quad (1)$$

where the thermal flux q is given by $q = -k \delta T / \delta r$, and k , ρ , C_p are thermal conductivity, density and specific heat of the ball; H is the heat evolution per unit volume. Equation (1) was integrated using spreadsheet software, with property values using the assumptions below. The temperature profiles at various times are flat, except for a sharp drop near the surface. Thus the interior of the ball is not affected by heat losses from the surface over the likely life of the ball. Figure 2 shows the central plateau temperature of a ball with diameter $D = 300 \text{ mm}$, formed from 25-nm spheres, as a function of time, for three starting temperatures. The exponential rise of H with temperature yields abrupt increases after around 3–30 s for starting temperatures of 1,400–1,200 K. Here the model predicts a violent end to the ball. As the temperature rises above 1,700 or 2,000 K, silicon or silica will melt, allowing faster oxidation and network break-up. But for lower reactive-metal loadings (for example, ball lightning from low-carbon soils), the melting temperature may not be reached, with the ball fading from view. For lower starting temperatures, the ball may become visible only over the later part of its lifetime, which could be after minutes, so that it is not easily connected with the formative lightning strike.

Radiation transfer is assumed to not significantly affect the energy balance of the ball (discussed below). The k of the ball is taken to be that of air, ignoring the solids contribution (there is little connected cross-section). Energy loss from the exterior is by natural convection. Energy dissipation H increases as the surface area of the nanospheres, using the early (constant) rate per m^2 for planar surfaces of silicon¹⁵. Any soot has been already oxidized shortly after ball formation. Nanoparticle SiO or SiC are not considered in these numerical results, but will oxidize like Si (if SiO, with a lower heat of oxidation²¹). Finally, H is not limited by diffusion of oxygen into the ball; that is, the mole fraction of oxygen gas remains constant at all ball radii (an excellent approximation at $<1,400 \text{ K}$).

The above assumptions give rates of external energy loss by convection of 20–40 W for a 300-mm ball once the inner temperature reaches around 1,450 K. The oxidation energy release rate is much higher (here 1,100 W), and is largely absorbed by heating the ball mass. The total chemical energy density is 3.3 MJ m^{-3} , lying within the very approximate observational estimates of 1.5–15 MJ m^{-3} for average ball lightning¹. A cool outer surface and lack of impression of (radiant) heat are natural outcomes of this model, corresponding to generally observed properties^{2,3}.

We now consider the effective luminosity. The simplest assumption is that the nanospheres emit or absorb according to optical properties of bulk materials. This is adequate for particles $>10 \text{ nm}$ diameter²². Rayleigh’s approximation²³ for the absorption cross-section of a sphere allows one to estimate the linear absorption coefficient, α_{abs} , of the nanosphere suspension for various wavelengths, using listed values of extinction coefficient κ and refractive index n for crystalline Si, crystalline SiO_2 and amorphous SiO (ref. 24). For 100 g m^{-3} Si in the form of Si, SiO or SiO_2 , the ball is optically transparent in the visible range (for Si at a wavelength of 600 nm, $\alpha_{\text{abs}} = 0.26 \text{ m}^{-1}$, so $\alpha_{\text{abs}} D = 0.08 \ll 1$), allowing one to sum the contributions of all nanoparticles for the ball emission. Emissivity is taken as equal to absorptivity.

The emission is the product of emissivity and the blackbody emission e_b for each wavelength λ ; this gives a sharp peak in the red part of the spectrum for both Si and SiO, because $d\kappa/d\lambda$ is negative and counters the positive $de_b/d\lambda$. At 1,200–1,400 K, 4.5–35 W is emitted from the whole Si peak, corresponding to 1.2–14 W over the

visible range 400–800 nm. A 100-W tungsten filament lamp (observed distribution median¹) emits 8 W in the visible (with its filament at 3,000 K), matching this nanosphere model at 1,350 K. The λ dependence of Si emission at 1,200 K matches a 1,700 K blackbody profile in the visible, so such a ball would be reported as ‘translucent white’. Lower temperatures may be reported as yellow or red, thus covering most of the observed colours. Optical emission may also come from molecules of salts vaporized from the soil. Many soils are expected to yield SiO rather than Si. Amorphous Si may also be formed, with a higher absorptivity than if crystalline²⁵. (We note that some lightning strikes (or man-made discharges) on metal structures may also result in a long-lived oxidation of networked metal nanospheres.)

The model of a nanoparticle network of slowly oxidizing Si that we present here successfully explains all the salient observed features of ball lightning in its most common environment. Future work may usefully explore the lightning/soil interaction, the chemical properties of the soil (or soil/wood mix) and lightning parameters (strength, duration), to find those which produce ball lightning in the laboratory. □

Received 1 September; accepted 10 November 1999.

- Smirnov, B. M. The properties and the nature of ball lightning. *Phys. Rep.* **152**, 177–226 (1987).
- Barry, J. D. *Ball Lightning and Bead Lightning* (Plenum, New York, 1980).
- Turner, D. J. The structure and stability of ball lightning. *Phil. Trans. R. Soc. Lond. A* **347**, 83–111 (1994).
- Singer, S. *The Nature of Ball Lightning* (Plenum, New York, 1971).
- Hutchison, S. G., Richardson, L. S. & Wai, C. M. Carbothermic reduction of silicon dioxide—a thermodynamic investigation. *Metall. Trans. B* **19**, 249–253 (1988).
- Essene, E. J. & Fisher, D. C. Lightning strike fusion: extreme reduction and metal-silicate liquid immiscibility. *Science* **234**, 189–193 (1986).
- Siegel, R. W. in *Physics of New Materials* 2nd edn (ed. Fujita, F. E.) 66–106 (Springer, Heidelberg, 1998).
- Ludwig, M. H. in *Handbook of Optical Properties* Vol. II, *Optics of Small Particles, Interfaces and Surfaces* (eds Hummel, R. E. & Wissmann, P.) 103–127 (CRC, Boca Raton, 1997).
- Friedlander, S. I., Jang, H. D. & Ryu, K. H. Elastic behaviour of nanoparticle chain aggregates. *Appl. Phys. Lett.* **72**, 173–175 (1998).
- Fortov, V. E. *et al.* Highly nonideal classical thermal plasmas: experimental study of ordered macroparticle structures. *JETP* **84**, 256–261 (1997).
- Aleksandrov, V. Ya., Borodin, I. P., Kechenko, E. V. & Podmoshenskii, I. V. Rapid coagulation of submicron aerosols into filamentary three-dimensional structures. *Sov. Phys. Tech. Phys.* **27**, 527–529 (1982).
- Cawood, W. & Patterson, H. S. A curious phenomenon shown by highly charged aerosols. *Nature* **128**, 150 (1931).
- Aleksandrov, V. Ya., Golubev, E. M. & Podmoshenskii, I. V. Aerosol mode of ball lightning. *Sov. Phys. Tech. Phys.* **27**, 1221–1224 (1983).
- Lowke, J. J., Uman, M. A. & Liebermann, R. W. Toward a theory of ball lightning. *J. Geophys. Res.* **74**, 6887–6898 (1969).
- Deal, B. E. & Grove, A. S. General relationship for the thermal oxidation of silicon. *J. Appl. Phys.* **36**, 3770–3778 (1963).
- Massoud, H. Z. & Plummer, J. D. Analytical relationship for the oxidation of silicon in dry oxygen in the thin-film regime. *J. Appl. Phys.* **62**, 3416–3423 (1987).
- Jacobson, N. S. Corrosion of silicon-based ceramics in combustion environments. *J. Am. Ceram. Soc.* **76**, 3–28 (1993).
- Rayle, W. D. *Ball Lightning Characteristics* (Note TND-3188, NASA, Washington, 1966).
- Andrianov, A. M. & Sinityn, V. I. Erosion-discharge model for ball lightning. *Sov. Phys. Tech. Phys.* **22**, 1342–1347 (1977).
- Pemberton, S. T. & Davidson, J. F. Turbulence in the freeboard of a gas-fluidized bed. The significance of ghost bubbles. *Chem. Eng. Sci.* **39**, 829–840 (1984).
- Nagamori, M., Boivin, J. A. & Claveau, A. Gibbs free energies of formation of amorphous Si₂O₃, SiO and SiO₂. *J. Non-Cryst. Solids* **189**, 270–276 (1995).
- Littau, K. A. *et al.* A luminescent silicon nanocrystal colloid via a high-temperature aerosol reaction. *J. Phys. Chem.* **97**, 1224–1230 (1993).
- Bohren, C. F. & Huffman, D. R. *Absorption and Scattering of Light by Small Particles* (Wiley, New York, 1983).
- Palik, E. D. *Handbook of Optical Constants of Solids* (Academic, Orlando, 1985).
- INSPEC *Properties of Silicon* 75, 938 (Institution of Electrical Engineers, London, 1988).

Acknowledgements

We thank the Electrical and Electronic Engineering Department at the University of Canterbury, especially J. Woudberg, for the use of their high-voltage laboratory; C. Maslin, B. Lane, P. Niamskul and T. Benson for experimental work, supporting that of J. Dinniss, and D. Brown, N. Foot and R. Boyce for technical help. We also thank N. Andrews and J. McKenzie of the Plant and Microbial Sciences Department for electron microscopy.

Correspondence and requests for materials should be addressed to J.A. (e-mail: j.abrahamson@cape.canterbury.ac.nz).

Large-scale complementary integrated circuits based on organic transistors

B. Crone*, **A. Dodabalapur***, **Y.-Y. Lin***, **R. W. Filas***, **Z. Bao***, **A. LaDuca†**, **R. Sarpeshkar*‡**, **H. E. Katz*** & **W. Li***

* Bell Laboratories, Lucent Technologies, 600 Mountain Avenue, Murray Hill, New Jersey 07974, USA

† Lucent Technologies, 555 Union Boulevard, Allentown, Pennsylvania 18103, USA

‡ Present address: Department of Electrical Engineering, Massachusetts Institute of Technology, Cambridge, Massachusetts 02139, USA

Thin-film transistors based on molecular and polymeric organic materials have been proposed for a number of applications, such as displays^{1–3} and radio-frequency identification tags^{4–6}. The main factors motivating investigations of organic transistors are their lower cost and simpler packaging, relative to conventional inorganic electronics, and their compatibility with flexible substrates^{7,8}. In most digital circuitry, minimal power dissipation and stability of performance against transistor parameter variations are crucial. In silicon-based microelectronics, these are achieved through the use of complementary logic—which incorporates both p- and n-type transistors—and it is therefore reasonable to suppose that adoption of such an approach with organic semiconductors will similarly result in reduced power dissipation, improved noise margins and greater operational stability. Complementary inverters and ring oscillators have already been reported^{9,10}. Here we show that such an approach can realize much larger scales of integration (in the present case, up to 864 transistors per circuit) and operation speeds of ~1 kHz in clocked sequential complementary circuits.

Our fabrication method for organic complementary circuits spatially separates n-channel and p-channel transistors to facilitate the separate deposition of electron-transporting and hole-transporting semiconductors. Other approaches are possible, and an alternative method will also be outlined. In the experiments described below, hexadecafluorocopper phthalocyanine (F-CuPc) is used as the n-type semiconductor and α -sexithiophene (α -6T) as the p-type semiconductor. The chemical structures of these

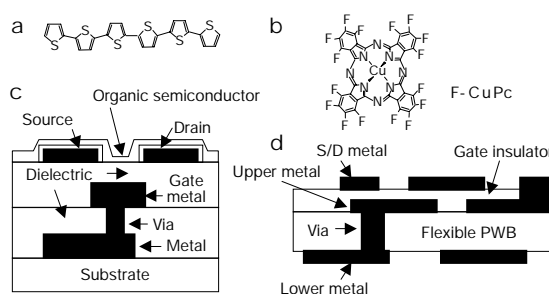


Figure 1 Chemical structures of organic semiconductors and schematic layer structures of circuits. **a**, Structure of α -sexithiophene (α -6T); **b**, structure of hexadecafluorocopper phthalocyanine (F-CuPc). **c**, Schematic layer structure of the circuits used in this study. The circuits are fabricated on rigid substrates, and metal lines and vias are defined by photolithography and standard semiconductor processing techniques. The interconnection metal level is defined immediately above the substrate, followed by the gate metal level and the source/drain (S/D) metal level. The interlayer dielectrics are not shown. The organic semiconductor is deposited above the S/D metal. **d**, Schematic of the cross-section of an organic transistor circuit technology based on flexible printed wiring boards.